33rd Annual International Conference of the IEEE EMBS
Boston, Massachusetts USA, August 30 - September 3, 2011

Model-based Optic Nerve Head Segmentation on Retinal Fundus Images

Fengshou Yin, Jiang Liu, Sim Heng Ong, Ying Sun, Damon W.K.Wong, Ngan Meng Tan, Carol Cheung, Mani Baskaran, Tin Aung, Tien Yin Wong

Abstract— **The optic nerve head (optic disc) plays an important role in the diagnosis of retinal diseases. Automatic localization and segmentation of the optic disc is critical towards a good computer-aided diagnosis (CAD) system. In this paper, we propose a method that combines edge detection, the Circular Hough Transform and a statistical deformable model to detect the optic disc from retinal fundus images. The algorithm was evaluated against a data set of 325 digital color fundus images, which includes both normal images and images with various pathologies. The result shows that the average error in area overlap is 11.3% and the average absolute area error is 10.8%, which outperforms existing methods. The result indicates a high correlation with ground truth segmentation and thus demonstrates a good potential for this system to be integrated with other retinal CAD systems.**

I. Introduction

The optic nerve head, or optic disc, is the location where the optic nerve connects to the retina [1]. It is also known as the blind spot as this area of the retina cannot respond to light stimulation due to the lack of photoreceptors. In a typical retinal fundus image, the optic disc is an elliptic region which is brighter than the surrounding region.

The features related to the optic disc such as optic disc size, disc tilting ratio, cup-to-disc ratio and peripapillary atrophy are important indicators of various ophthalmic pathologies. For instance, optic disc size and cup-to-disc ratio are important risk factors for the diagnosis of glaucoma. In pathological myopia, smaller disc tilting ratio and existing of peripapillary atrophy indicate high possibility of pathological myopia. Thus, correct localization and accurate segmentation of the optic disc play an important role in computer aided diagnosis systems.

Much work has been done to locate the optic disc and several studies have been published on the segmentation of the optic disc. Lowell et al. [2] employed a specialized template matching for disc localization and a circular deformable model for segmentation. Aquino et al. [3] used morphological and edge detection techniques together with Circular Hough Transform to estimate the disc boundary. Kim et al. [4] made use of warping and random sample consensus (RANSAC) to segment the optic disc. Wong et al. [5] proposed a method based on the level set method followed by ellipse fitting to smooth the disc boundary. Abramoff et al. [6] detected the optic disc by a pixel classification method using the feature analysis and nearest neighbor algorithm. Muramatsu et al. [7] compared the active contour model with two pixel classification methods – fuzzy c-means clustering and artificial neural networks, and concluded that the performance of these three methods were similar.

In this paper, we introduce an automatic optic disc segmentation method based on statistical deformable model approach. Edge detection and the Circular Hough Transform (CHT) are combined with an active shape model to extract the optic disc boundary. In particular, we will discuss how the algorithm works to improve the optic disc segmentation. Algorithm performance will be obtained by testing it on a large population based database.

II. Method

The proposed method deploys the active shape model (ASM) framework [8] using color retinal fundus images. The general shape and appearance of the optic disc are modeled in the training stage. To process a new image, a pre-processing step is utilized to analyse the image and choose the optimal channel to be processed. The statistical shape model is then initialized by an estimation of the optic disc size and location by edge detection and CHT. The final contour of the optic disc is obtained by deforming the model in multi-resolution until the stopping criterion is met.

A. Shape and Appearance Modeling

The Point Distribution Model (PDM) models the shape by a series of landmark points, and it is used in the shape modeling of our algorithm. A 2D shape which is represented by m landmark points $(x_1, y_1),...(x_m, y_m)$ can be denoted by

$$\mathrm{x} = (x_1, y_1, ..., x_m, y_m)^T \tag{1}$$

To build a robust PDM, a large training set is needed. All the landmarked shape vectors should be aligned to each other by scaling, rotation and translation until the complete training set is properly aligned. The aim of aligning the training shapes is to minimize the weighted sum of squared distances.

The mean shape and covariance of the aligned shapes can be computed by

$$\bar{\mathrm{x}} = \frac{1}{n}\sum_{i=1}^{n} \mathrm{x}_i \tag{2}$$

and

$$\mathrm{S} = \frac{1}{n-1}\sum_{i=1}^{n} (\mathrm{x}_i - \bar{\mathrm{x}})(\mathrm{x}_i - \bar{\mathrm{x}})^T \tag{3}$$

This work was supported in part by the Agency for Science, Technology and Research, Singapore, under SERC grant 092-148-00731.

Fengshou Yin, Jiang Liu, Damon W.K. Wong and Ngan Meng Tan are with the Institute for Infocomm Research, A*STAR, Singapore (e-mail: fyin@ i2r.a-star.edu.sg).

Sim Heng Ong and Ying Sun are with the National University of Singapore.

Carol Cheung, Mani Baskaran, Aung Tin and Tien Yin Wong are with the Singapore Eye Research Institute. Tien Yin Wong is also with the National University of Singapore.

respectively, where n represents the number of shapes in the training set. By applying principal component analysis (PCA), the major dimensions can be identified by corresponding them to the eigenvalues. Suppose the first t eigenvectors are stored in the matrix $\Phi = (\phi_1 | \phi_2 | ... | \phi_t)$, a shape can now be approximated by

$$\mathrm{x} \approx \bar{\mathrm{x}} + \Phi \mathrm{b} \tag{4}$$

where

$$\mathrm{b} = \Phi^T (\mathrm{x} - \bar{\mathrm{x}}) \tag{5}$$

is a vector of t elements containing the model parameters.

The largest eigenvalues are chosen to explain a certain percentage f_v of the variance in the training shapes. Therefore, t is the smallest number for which

$$\sum_{i=1}^{t} \lambda_i \geq f_v \sum_{i=1}^{2n} \lambda_i \tag{6}$$

In our algorithm, the number of landmark points is set to be 24, and the value of t is chosen to be the number that can explain 99% of the total variance.

The gray-level appearance model describes the typical image structure surrounding each landmark point. The model is obtained from pixel profiles sampled around each landmark point, perpendicular to the line that connects the neighboring points. The appearance model is built using the normalized first derivatives of these pixel profiles. Denoting the normalized derivative profiles as $g_1, ..., g_s$, the mean profile $\bar{g}$ and the covariance matrix S_g can be computed for each landmark. The model for the gray levels around each landmark is represented by $\bar{g}$ and S_g.

B. Pre-processing

The interweaving of blood vessels is one of the major obstacles for accurate disc segmentation. Thus, a proper pre-processing step is necessary to reduce the impact of blood vessels. For digital color fundus images, the red channel component has the least information about the blood vessels in the disc region, followed by the blue channel. Therefore, the red component is preferred in the model fitting process. However, the red component of some images is evenly distributed and the disc region cannot be identified through this channel. In such cases, blue channel component is used instead. To choose the proper channel image, we use a voting scheme based on heuristics. Denoting the red, green, blue and grey images by I_r, I_g, I_b and I_{grey} respectively, the optimal image I_{op} can be chosen by

$$I_{op} = \begin{cases} I_r & if\ mean(I_r) \leq TH \\ I_b & if\ mean(I_r) > TH \end{cases} \tag{7}$$

where $mean(I_r)$ is the average intensity of the red channel image, and TH is the threshold value for determining the optimal image. Fig. 1 shows examples of the optimal channel selection.

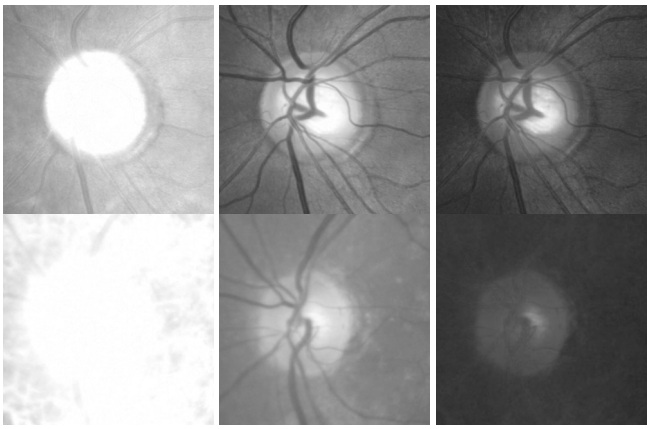

Fig. 1. Different channels of fundus image: from left to right, red, green, blue. Upper row: red channel as the optimal image. Lower row: blue channel as the optimal image.

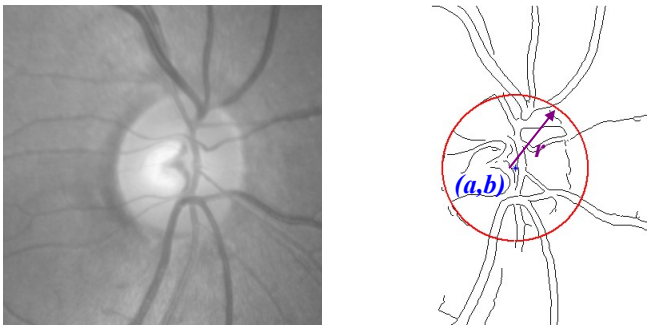

Fig. 2. (a) Greyscale image (b) Edge map of (a) and the estimated circular disc by CHT

C. Edge Detection and Circular Hough Transform

Initialization is a critical step for any deformable models. A good initialization can avoid the problem of local maxima/minima and reduce the computing time. In case of optic disc segmentation, a good initialization would locate the disc center and estimate the disc size for each image. We estimate the position and size of the optic disc using an edge -based method. The Canny edge detector [9] is used to obtain the edge map of the grayscale image.

The optic disc can be approximated by a circle in the fundus image. The knowledge-based Circular Hough Transform is used to detect a circle that can best estimate the optic disc with appropriate disc diameter range. A circle can be represented in the parametric form as

$$(x-a)^2 + (y-b)^2 = r^2 \tag{8}$$

where (a,b) is the center of the circle and r is the radius. The circle shapes that exist in the edge map can be found by performing the Circular Hough Transform in the following way:

$$(a,b,r) = CHT(I_{em}, r_{\min}, r_{\max}) \tag{9}$$

where I_{em} is the edge map of the optimal image. $r_{\min}$ and $r_{\max}$ are the minimum and maximum radius limits for the circle search. The constraint on the minimum radius is to eliminate the effect of random edges that can form a small circle while the constraint on the maximum radius can reduce the chances of detecting spurious large circles that maybe caused by the

existence of peripapillary atrophy. Fig 2 shows an example of this step.

D. Optic Disc Boundary Extraction

After obtaining the estimation of the optic disc center and diameter from the previous step, we can initialize the statistical deformable model to fine-tune the disc boundary according to the image texture. The initial shape can be represented by a scaled, rotated and translated version of the reference shape $\overline{\mathrm{x}}$:

$$\mathrm{x} = M(s,\theta)[\overline{\mathrm{x}}] + T \tag{10}$$

where $M(s,\theta)$ is the scaling and rotation matrix, and T is the translation vector. In optic disc segmentation, rotation of the shape cannot be predicted for a new image. Thus, the initial shape is estimated by the scaled and translated version of the mean shape of the model. The scaling ratio can be obtained by taking the ratio of the diameter of the circle in the previous step over the disc diameter in the mean shape. The translation can be calculated by the vector between the center of model and the center of the circle approximated in the previous step by CHT.

The evolving process of the active shape model can be constructed for multiple resolutions. The best resolution uses the original image with a step size of one pixel when sampling the profiles. The next resolution is the image that halves the size of the original image and with a double step size. Subsequent levels are obtained by halving the image size and doubling the step size. Multi-resolution image search can not only reduce the number of computations but also enhance segmentation accuracy. Low-resolution images are used to search points that are far from the desired position based on global image structures, and high-resolution images are used to search near points for refinement of the segmentation result.

Starting from the mean shape, the models are fitted in an iterative manner. Each model point is moved toward the direction perpendicular to the contour. The new landmark position can be obtained by minimizing the following Mahalanobis distance

$$f(g_i) = (g_i - \overline{g})S_g^{-1}(g_i - \overline{g}) \tag{11}$$

The updated segmentation can be obtained after all the landmarks are moved to new positions. This process is repeated by a specified number of times at each resolution, in a coarse-to-fine fashion.

Due to the limited number of landmark points, the obtained contour is usually not smooth. The direct least squared ellipse fitting method is used to smooth the boundary of the optic disc [10].

III. Experimental results

The ORIGA^{light} database [11] which consists of 650 images is used to test our algorithm. The images are from the Singapore Malay Eye Study (SiMES) database, a population-based study of eye diseases for the Malay population over 40 years old in Singapore. The optic disc boundary was manually marked by a group of experienced graders from Singapore Eye Research Institute. Group consensus was reached for each image, and it is used as the ground truth. The segmentation only relies on the information from the retinal fundus image without additional clinical data.

To test our algorithm, we divided the database randomly into two sets with 325 images in each set. The first set was used to train the optic disc model, and the second set was used to test the performance of the algorithm. We also implemented the level set based method in [6], fuzzy c-means (FCM) clustering based method in [7] and CHT based method for comparison purposes.

To quantify the performance of our algorithm, a number of performance metrics were used. The area overlap error [12] is defined as

$$m_1 = (1 - \frac{Area(S \bigcap R)}{Area(S \bigcup R)}) \times 100\% \tag{12}$$

where S is the mask of our segmented result and R is the mask of the ground truth segmentation. This performance metric indicates how well the segmented result matches with the ground truth, where m_1 =0 indicates perfect match of the segmented result with the ground truth and m_1 =1 indicates no overlap. Although area overlap error is an important metric for segmentation performance, it fails to indicate whether the result is over or under segmented. Thus, the relative area difference (m_2) metric is used to complement the area overlap error. It is defined as

$$m_2 = \frac{Area(S) - Area(R)}{Area(R)} \times 100\% \tag{13}$$

The relative area difference indicates whether the segmentation is over or under segmented by its sign, where a negative sign denotes under-segmentation and a positive sign denotes over-segmentation. Similar to the area overlap error, a m_2 value of '0' indicates no area difference between segmented result and the ground truth.

To measure the degree of mismatch of contour points, the Hausdorff distance was calculated. The Hausdorff distance [13] is defined as

$$H(A,B) = \max(h(A,B), h(B,A)) \tag{14}$$

where $A = \{a_1, a_2, ..., a_m\}$ and $B = \{b_1, b_2, ..., b_n\}$ are two sets of contour points and

$$h(A,B) = \max_{a \in A} \min_{b \in B} \| a - b \| \tag{15}$$

with $\| a - b \|$ representing the Euclidean distance between a and b .

The results of our proposed method and the other three methods are summarised in Table I.

TABLE I. SUMMARY OF RESULTS

Metric \ Method	Proposed Method	FCM Method	CHT Method	Level set Method
m_1 mean	11.3%	25.2%	25.5%	23.1%
m_2 mean	>0	>0	>0	>0
$\|m_2\|$ mean	10.8%	38.4%	19.0%	29.9%
Hausdorff Distance(px)	27	68	56	78

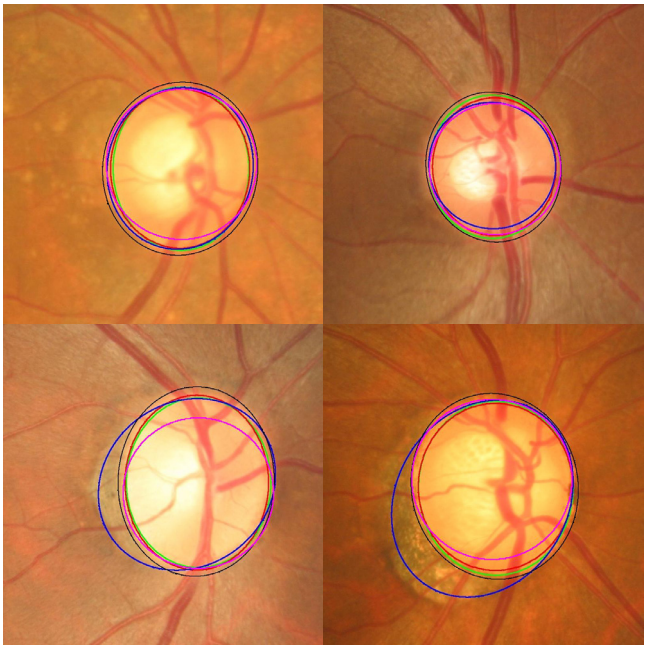

Fig. 3. Examples of optic disc segmentation using the proposed method (red), level set method (blue), FCM method (black), CHT method (cyan) and ground truth (green)

From the table, we see that the proposed method performs better than the level set method, FCM clustering method and CHT method in terms of overlap error, absolute area error and Hausdorff distance. The average value of m_1 for the proposed method is 11.3%, which improves significantly compared to the m_1 value of over 20% for the other three methods. All four methods generally over segment the optic disc as shown by positive m_2 values. The mean absolute area error can achieve as low as 10.8% for the proposed method while the best performance for the other methods is 19.0%. The Hausdorff distance for the proposed method is also much lower than other methods. Fig. 3 lists some examples of the segmentation results for all four methods.

The level set method searches the whole ROI for the optic disc and it is easily trapped by strong edges. As shown in the segmentation results, the level set method usually over-segments the optic disc as the evolution stops at the blood vessel boundary or peripapillary atrophy boundary instead of disc boundary. In FCM clustering method, the performance depends heavily on the inputs to the unsupervised classifier as well as the number of clusters specified. The CHT method performs well on images with circular shaped optic disc. However, the results can be much worse for discs with non-circular shapes. The proposed method performs better than these three methods for two reasons. First, the robust initialization method provides an accurate estimation of the size and location of the optic disc, resulting in minimal local refinement of the contour. Second, statistical deformable model can refine the disc boundary more accurately due to its pre-determined direction and extent of evolution by training.

IV. Conclusions

In this paper, we have proposed an automatic method to segment the optic disc from fundus images using statistical deformable model approach. Experimental results on a large database show that the proposed method performs better than many existing methods. The results are promising for a population based database consisting of images with multiple pathologies. Thus it demonstrates good potential for our method to be used to aid the diagnosis of retinal diseases.

References

[1] W. Tasman and E. A. Jaeger, Duane's Ophthalmology, Lippincott Williams & Wilkins, (2006)

[2] J. Lowell, A. Hunter, D. Steel, A. Basu, R. Ryder, E. Fletcher and L. Kennedy, "Optic Nerve Head Segmentation" L., *IEEE T. Med Imag*, Vol. 23, No. 2, 256-264 (2004)

[3] A. Aquino, M. Gegundez-Arias and D. Marin, "Detecting the Optic Disc Boundary in Digital Fundus Images Using Morphological, Edge Detection and Feature Extraction Technique", *IEEE T. Med Imag*, Vol. PP, Issue 99 (2010)

[4] S.K. Kim, H.J. Kong, J.M. Seo, B.J. Cho, H. Chung, K.H. Park, D.M. Kim, J.M. Hwang and H.C. Kim, "Segmentation of Optic Nerve Head using Warping and RANSAC", *Conf Proc IEEE Eng Med Biol Soc* 2007, 900-903 (2007).

[5] D.W.K. Wong, J. Liu, J.H. Lim, X. Jia, F. Yin, H. Li and T.Y. Wong, "Level-set based automatic cup-to-disc ratio determination using retinal fundus images in ARGALI", *Conf Proc IEEE Eng Med Biol Soc*.2008; 2266-9(2008)

[6] M.D. Abramoff, W.L.M. Alward, E.C. Greenlee, L. Shuba, C.Y. Kim, J.H. Fingert and Y.H. Kwon, "Automated segmentation of theoptic disc from stereo color photographs using physiologically plausible features", *Invest. Ophthalmol. Vis. Sci*. 48, 1665–1673(2007).

[7] C. Muramatsu, T. Nakagawa, A. Sawada, Y. Hatanaka, T. Hara, T. Yamamoto and H. Fujita, "Automated segmentation of optic disc region on retinal fundus photographs: Comparison of contour modeling and pixel classification methods " , *Computer Methods and Programs in Biomedicine* - January 2011 (Vol. 101, Issue 1, Pages 23-32

[8] T. Cootes, C. Taylor, D. Cooper and J. Graham, "Active Shape Models - Their Training and Application", *Computer Vision and Image Understanding*, Vol. 61, No. 1, 38-59 (1995).

[9] J. Canny, "A Computational Approach to Edge Detection," *IEEE Transactions on Pattern Analysis and Machine Intelligence*,Vol. PAMI-8, No. 6, 1986, pp. 679-698.

[10] A. Fitzgibbon, M. Pilu, and R. B. Fisher, "Direct Least Square Fitting of Ellipses". *IEEE Transactions On Pattern Analysis and Machine Intelligence*, Vol. 21, No. 5, May 1999

[11] Z. Zhang, F. Yin, J. Liu, D.W.K. Wong, N.M. Tan, B.H. Lee, J. Cheng and T. Y. Wong, "ORIGA-light: An online retinal fundus image database for glaucoma analysis and research," *Conf Proc IEEE Eng Med Biol Soc*., pp.3065-3068, Aug. 31 2010-Sept. 4 2010

[12] D. Xiang and G. Du: Editorial: 3D Segmentation in the Clinic: A Grand Challenge II -Liver Tumor Segmentation. MICCAI 2008.

[13] G. Rote, "Computing the minimum Hausdorff distance between two point sets on a line under translation", *Information Processing Letters*, v. 38, pp. 123-127.